Fast Decision in Favor of the Slow Fission Process

V. Tishchenko,[1,*] C.-M. Herbach,[1] D. Hilscher,[1] U. Jahnke,[1,†] J. Galin,[2] F. Goldenbaum,[3] A. Letourneau,[2] and W.-U. Schröder[4]

[1]*Hahn-Meitner-Institut Berlin, Glienickerstrasse 100, D-14109 Berlin, Germany*
[2]*GANIL (IN2P3-CNRS, DSM-CEA), BP 5027, F-14076 Caen-Cedex 5, France*
[3]*Institut für Kernphysik, Forschungszentrum Jülich GmbH, D-52428 Jülich, Germany*
[4]*University of Rochester, Rochester, New York 14627, USA*

(Received 3 May 2005; published 11 October 2005)

The fission probability P_f of highly excited targetlike nuclei produced in reactions of 2.5 GeV protons on Au, Bi, and U was studied as a function of excitation energy E^* whereby E^* is deduced eventwise from the multiplicity of evaporated light particles. At the highest E^* of 1000 MeV P_f amounts to $\approx 30\%$ with all 3 target nuclei irrespective of the initial fissility. Statistical-model calculations satisfactorily reproduce the observed evolution of P_f with E^*—provided that no extra transient delay is introduced. Fission thus is decided upon very fast and early in the long deexcitation chain towards scission which comprises as much as $\approx 80\%$ of all evaporated alpha particles.

DOI: 10.1103/PhysRevLett.95.162701 PACS numbers: 24.75.+i, 24.10.−i, 25.40.Sc, 24.60.Dr

At low excitation energy nuclear fission is strongly influenced by nuclear shell effects, resulting, for instance, for U in the well known binary split into two mass asymmetric fission fragments. With increasing excitation these nuclear structure effects are washed out, and macroscopic properties such as nuclear dissipation dominate the collective flow of nuclear matter from the equilibrium deformation via the saddle towards scission into two fragments of about equal size. The overall time elapsed from the equilibrium deformation up to scission is found to be a few times 10^{-20} s. This time is quite long compared to other processes such as the emission of neutrons which is 10 to 100 times faster. This observation has led to the notion of fission being a slow process [1].

Since the magnitude of nuclear dissipation is most likely deformation dependent [2], the characteristic time governing the flow over the saddle point, where the decision about fission is made, might be considerably shorter than the one close to the scission point. In particular, at high excitation energies, where the emission times of light charged particles are very short, a long transient delay for fission at the saddle point would strongly favor the emission of charged particles, thus reducing the fissility and, consequently, second- and higher-chance fission probabilities. Conversely, low dissipation at the saddle or a minimum transient delay tends to keep fission competitive with particle evaporation even at high excitation. In other words, although the entire fission process is slow, the decision to fission can be fast.

We have chosen 2.5 GeV proton-induced reactions to excite three target nuclei, Au, Bi, and U with different fissilities $Z^2/A = 31.7$, 33.0, and 35.6, respectively, in order to study the evolution of the inelastic reaction, σ_{inel}, and the fission cross section, σ_f, as a function of excitation energy, E^*, *and* fissility. Their ratio, the fission probability $P_f(E^*) = \sigma_f(E^*)/\sigma_{\text{inel}}(E^*)$, provides the best possible evidence for the presence of dissipative or transient effects in fission. The selected reactions, similar to antiproton [3,4] or peripheral relativistic heavy-ion reactions [5,6], are thought to deposit high thermal excitation with minimum ballast from collective excitations (angular momentum, shape distortions, or compression) which could have a detrimental influence on the decay.

The maximum E^* reached in the present investigation is only about 4–5 MeV/nucleon or $\approx$1000 MeV, as will be shown below. This excitation is well below that reported for the onset of multifragmentation [7], the decay of a hot nucleus into multiple clusters and nucleons. Thus the two main reaction channels expected are spallation induced fission and evaporation, the latter process leading to the survival of a heavy targetlike residue (HR) plus many evaporated neutrons and light charged particles (LCPs).

The amount of energy dissipated into excitation is deduced event by event from the total number of evaporated light particles (n, H, He), a well proven technique, the details of which are described in [8,9]. It presupposes a 4π coverage and high acceptance at high granularity of the detectors, requirements fulfilled by the combination of our two detectors, the Berlin Neutron Ball (BNB) and the Berlin Silicon Ball (BSiB). BNB is a large spherical tank with 1500 l of Gd-loaded scintillator liquid, which in its central reaction chamber houses the BSiB, a self-supporting shell of 151 individual Si detectors. These Si detectors provide a total geometrical acceptance of about 80% with their energy thresholds as low as 2 MeV.

The experiment was performed at the COSY accelerator in Jülich with targets of Au (2×324 μg/cm^2), Bi (629 μg/cm^2), and UF_4(725 μg/cm^2) + C(36 μg/cm^2). The hardware threshold of BNB was adjusted to detect all reactions with an inelasticity larger than 3 MeV. The high ($\approx$85%) detection efficiency of BNB for slow neutrons and the low ($\approx$15%) efficiency for energetic ($\gtrsim$100 MeV)

ones makes BNB sensitive rather to evaporative neutrons than to fast ones from the direct interaction of the incident proton with the target nucleus. In BSiB the identification of LCPs and the reconstruction of the mass of heavier fragments, i.e., of intermediate-mass fragments (IMFs), fission fragments (FFs), and HRs, are based on the measurement of time of flight and energy.

While the excitation energy, E^*, can be deduced from the experiment, the A and Z content of the excited nucleus after the fast intranuclear cascade (INC) is accessible from INC calculations only. Since the knowledge of A and Z is necessary for the calculation of P_f, the reliability of the employed INC model needs to be ascertained by comparing calculated *inclusive* E^* distributions with the data. Such a comparison is made in Fig. 1 exhibiting, indeed, a good agreement for the three target nuclei between experiment and the simulation with the INCL2.0 model from Cugnon [10]. We conclude that also the A, Z population is correctly described by the model.

The mass resolution in BSiB is relatively poor, in particular, for the heavier fragments, chiefly due to the short flight path of only 10 cm. Setting limits on the total mass of *all detected* reaction products, A_{tot}, and on the mass of the heaviest, A_1, and second heaviest particle, A_2, allows one to separate the three major fragmentation products HRs, FFs, and IMFs, as is illustrated in Fig. 2(a). It exhibits, for the case of Bi as an example, the correlation between A_1 and A_2. For the purpose of this plot, the experimental A_1-A_2 data have been symmetrized. Here, the events with both FFs detected are centered in the middle at $A_1, A_2 \approx 80$. Events with a HR detected together with some lighter masses appear close to the x and y axes near $A_1, A_2 \approx 150$, while most of the events with only one FF and some lighter masses detected are suppressed by the requirement $A_{tot} > 70\%$ of A_{targ}. Also, as expected, there are hardly any multifragmentation events, which would populate the lower left corner of the plot with $A_1, A_2 \lesssim 30$. In order to separate events with two FFs detected from HR events we use the further condition $A_1, A_2 > 32$ indicated by the dashed lines.

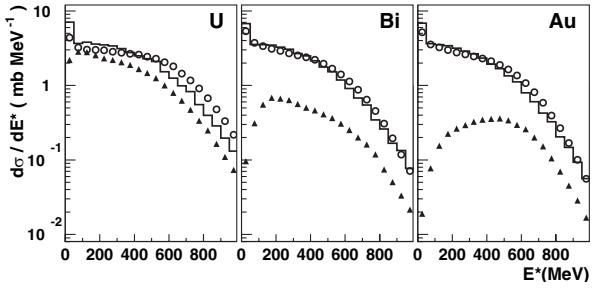

FIG. 1. Measured inelastic or inclusive (○) and fission (▲) differential cross sections $d\sigma/dE^*$ as a function of E^* for p(2.5 GeV) + U, Bi, and Au. The histograms show the result of INCL2.0 [10] calculations of the inclusive cross sections.

The two other panels in Fig. 2 are meant to demonstrate that fission events selected according to the above criteria also fulfill the more conventional conditions on the total kinetic energy (TKE) and the folding angle between the FFs. Indeed, Fig. 2(b) shows that these events are grouped around the solid line calculated with the Viola formula $\langle \mathrm{TKE} \rangle = 0.1189\ Z^2/A^{1/3} + 7.3$ MeV [11] with $Z = 0.45(A_1 + A_2)$, whereas they lie somewhat above the dashed line with Z values chosen according to the β stability—in agreement with other investigations [12]. As to the folding angle distribution plotted in Fig. 2(c), we witness a growing broadening and deviation from 180° with increasing E^* as the result of more and more numerous emission of lighter particles and increasing momentum transfer. Because of this strong evolution with E^*, we refrained from choosing a limiting folding angle.

Once the FFs have been selected with the two conditions $A_{tot} > 70\%$ of A_{targ} and $A_1 \geq A_2 > 30$, 32, and 35 for Au, Bi, and U, respectively, their yield is corrected for detection efficiency as described in Ref. [9] to give $\sigma_f(E^*)$, shown in Fig. 1 as a function of E^*. The total fission cross sections deduced amount to $\sigma_f = 200 \pm 60$ mb, 320 ± 50 mb, and 1350 ± 120 mb for Au, Bi, and U, respectively, in reasonable agreement with previous measurements [13]. The fission probability is then obtained directly as the ratio $P_f(E^*) = \sigma_f(E^*)/\sigma_{inel}(E^*)$. The evolution of P_f with E^* is shown in Fig. 3 for Au (○), Bi (●), and U (▼).

The figure shows that the evolution of $P_f(E^*)$ with E^* is quite different for the three targets. At the low excitation of about 150 MeV, the fission probability of a U-like nucleus is close to 90%, while for the less fissile Bi-like nucleus it is 25% and only 5% for Au-like nuclei. At such low E^*, the excited nuclei are still similar in A and Z to the target nucleus since only a few nucleons are removed during the INC stage, and the different behavior of $P_f(E^*)$ is still dominated by the different initial fissility. At higher E^*, considerably more nucleons are emitted during the INC (at

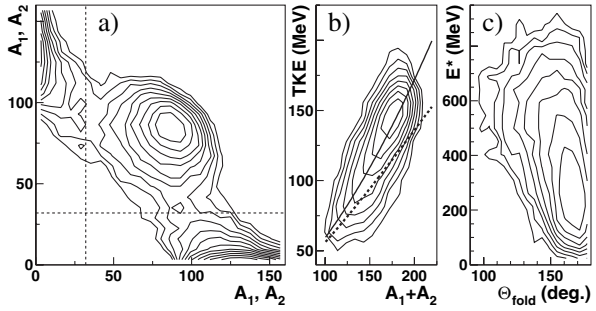

FIG. 2. Logarithmic contour plots used for the selection of fission fragments from the reaction p + Bi. (a) Correlation between the two heaviest fragments A_1 and A_2. (b) Total kinetic energy (TKE) of the two FFs as a function of their sum mass $A_1 + A_2$. (c) Distributions of the folding angle θ_{fold} between the FFs (in arbitrary units/rad) as a function of E^*.

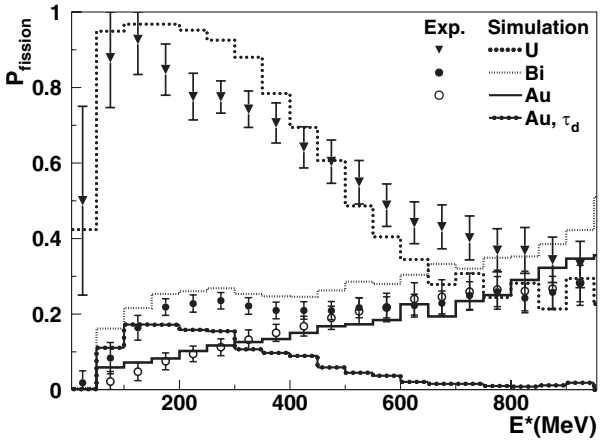

FIG. 3. Comparison of experimental (symbols) and simulated (histograms) fission probability as a function of E^*. The association with the three target nuclei is given in the figure. The simulation for p + Au with $a_f/a_n = 1.05$ and $\tau_d = 2 \times 10^{-21}$ s according to Ref. [5] is shown by the dot-dashed histogram.

$E^* = 1000$ MeV about $\Delta A = 12$ mass and $\Delta Z = 4$–5 charge units according to the INCL2.0 model [10], very similar for Au, Bi, and U). Consequently, the fissility of the thus produced nuclei is considerably lowered. This results in a strong decline of $P_f(E^*)$ in the case of U from the high value of about 90% at 150 MeV down to 35% at 900 MeV, while for the Au target a continuous increase of $P_f(E^*)$ with E^* is observed. For the Bi target one notices an intermediate behavior, with an almost constant value of about 25% between 200 and 600 MeV, followed by a further increase to 30%. Obviously, in the flat region of $P_f(E^*)$ for Bi the loss in fissility from the A, Z depopulation is compensated by an enhancement of fission due to the increase of E^*, while from then on the effect of an increasing E^* dominates.

Despite the large differences in fissility and fission barriers $B_f \approx 5$, 12, and 21 MeV (finite-range fission barriers [14] used in the calculations discussed below) of the initial nuclei U, Bi, and Au, respectively, one observes that $P_f(E^*)$ assumes the *same* value of about 30% for all three target nuclei at the highest excitations.

After this empirical discussion we confront now the observed evolution of P_f with E^* with statistical-model calculations applying the transition-state model to fission. To this purpose we have used the population of nuclei as a function of E^* predicted by the INCL2.0 code [10] as input to the statistical-model code GEMINI by Charity *et al.* [15]. The angular momentum imparted during the INC (up to 20 units of $\hbar$ at the highest E^*) is likewise taken into account. For the level density parameters we assumed $a_n = (A/10)$ MeV^{-1} and for their ratio at the transition state and at ground state deformation $a_f/a_n = 1.000$, 1.017, and 1.022 for U, Bi, and Au, respectively. For U and Au these values are the same as in [3], while for Bi we have chosen an intermediate value. No extra transient time for fission is applied. The result of these calculations is shown in Fig. 3 for the three targets by the dashed (U), dotted (Bi), and solid (Au) histograms. It is obvious that the calculations reproduce the characteristically different trends in P_f at lower E^*, as well as the almost equal P_f at the highest E^* nearly quantitatively, and, most importantly, they do so without the use of any additional transient time.

What can be learned from this agreement for the understanding of fission? From the calculations we can identify the range of multiple-chance fission steps or the range in excitation energy E^*_{fis} when fission is decided upon. At $E^* = 800$ MeV of initial excitation, for example, fission occurs at a mean excitation energy of $\langle E^*_{fis} \rangle = 700$ MeV for Au and Bi with a width of $\sigma_{E^*_{fis}} = 110$ MeV, while for U the corresponding values are 600 and 180 MeV. This implies that fission occurs rather early in the long deexcitation chain at these high initial excitation energies. For U, because of its lower fission barriers, fission is spread over a larger range of deexcitation steps and thus comes on average on a lower energy $\langle E^*_{fis} \rangle$.

These conclusions are at variance with the findings of Jurado *et al.* [6] reporting a *maximum* excitation energy for the decision to fission of less than 300 MeV in the reaction U (1A GeV) on $(CH_2)_n$. Also, Benlliure *et al.* [5] concluded from a similar inverse-kinematics experiment [Au (0.8A GeV) $+p$] on a *mean* energy for fission of $\langle E^*_{fis} \rangle = 128 \pm 20$ MeV for Au-like nuclei. These relatively low excitation energies were accounted for [5,6] in the calculations by a dynamical fission hindrance or a transient time of $\tau_d = 2 \times 10^{-21}$ s, which suppresses fission at higher E^*, and the resulting losses in σ_f were then compensated for by a relatively large value of the level density at saddle of $a_f/a_n = 1.05$.

In order to confront our data with these parameters, we show the thus calculated fission probability $P_f(E^*)$ for Au, as an example, by the dot-dashed line in Fig. 3. Clearly, this calculation fails to describe the actual Au fission data. It also fails in the case of Bi and U fission. This example also demonstrates the decisive advantage of the differential observation of $dP_f(E^*)/dE^*$ over other methods [5,6] in that it allows an *independent* determination of a_f/a_n and τ_d: a_f/a_n accounts for the rise of P_f at low $E^* \lesssim 200$ MeV, while τ_d becomes all the more effective the higher E^* is in excess of ≈ 300 MeV, i.e., the range which is fully covered with the present incident energy of 2.5 GeV, but much less so at 0.8 or 1 GeV [5,6].

The reason for the significant deviation of the present conclusions from those reported in Refs. [5,6] is not due to different model calculations. The INC/statistical-model calculations agree quite well when fed with the same parameters. Rather, the disaccord arises from the experiment. Since it is hardly possible to determine E^* in inverse kinematics directly from the number of evaporated particles, E^* is, instead, deduced [5,6] from the FFs' charges $Z_{1,2}$ and their distributions. There are, however, question-

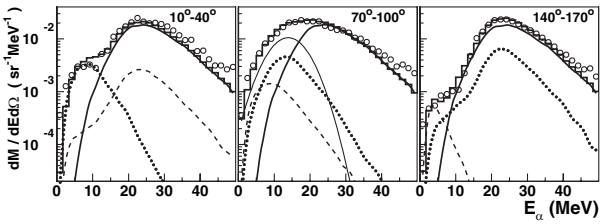

FIG. 4. Energy spectra of α particles that are emitted into 3 angular domains relative to the motion of the light fission fragment: $\Theta_{\alpha\text{-LF}} = 10^{\circ}$ to 40°, 70° to 100°, and 140° to 170°. Three calculated components are fitted to the experimental distribution (circles): the contribution from the compound nucleus prior to scission (thick continuous lines) and from the light (dashed lines) and the heavy (dotted lines) fission fragment. At 70° to 100° a further component for the neck emission is added (thin line). The total calculated spectrum is shown by the histogram. Example from 2.5 GeV p + Au at $E^* = 600$–900 MeV.

able assumptions and uncertain parameters involved in this delicate relation between $Z_{1,2}$ and E^* that shed serious doubts on the precision of the thus deduced E^* required for a convincing conclusion about τ_d.

The first part of the present investigation has shown that fission is initiated on a fast time scale and, hence, at high excitation. If this conclusion is correct, the large amount of remaining excitation must be carried off, either during the descent from saddle to scission or after scission. Indeed, according to the calculation at $E^* = 800$ MeV, only between 11% (Au) and 23% (U) of all light particles are emitted before reaching the saddle, or, more directly in terms of presaddle and postsaddle LCP multiplicities, $M^{\text{LCP}}_{\text{presaddle}} = 1.9, 1.9, 3.3$ and $M^{\text{LCP}}_{\text{postsaddle}} = 11.0$, 10.4, and 7.6 for Au, Bi, and U, respectively.

While from the present experiment the presaddle LCP emission cannot be disentangled from the postsaddle LCP emission, the amount of the *postscission* LCP emission can be deduced from their angular correlation with the fission axis. To this end we show in Fig. 4 the energy spectra of α particles (with a 10% admixture of ^{3}He) for three ranges of emission angles $\Theta_{\alpha\text{-LF}} = 10^{\circ}$–40°, 70°–100°, and 140°–170° relative to the motion direction of the light FF. The spectra are plotted in the center-of-mass system of the FFs from the reaction p + Au at $E^* = 600$–900 MeV, as an example. They are fitted with the predicted contributions from three relevant emission sources: from the compound nucleus prior to scission which is unrelated to the scission axis and from the two FFs which vary in shape and intensity with $\Theta_{\alpha\text{-LF}}$. At 70°–100°, i.e., perpendicular to the scission axis, it turned out to be necessary—in agreement with previous observations [16]—to add a small ($\approx$5% of the total α evaporation) component for neck emission which peaks at 15 MeV. The sum of all components shown by the histograms provides a good approximation at least to the lower-energy ($E_\alpha \lesssim 35$ MeV) part, i.e., to the evaporation part, of the spectra. This is, in particular, true for their low-energy shoulders visible near $E_\alpha = 5$ MeV due to the emission from the heavy (10°–40°) or the light (140°–170°) FF. The high-energy tails in the measured spectra, instead, originate partly from preequilibium α emission. From the good fit in the evaporation regime one concludes that as much as about 80% of the total evaporation yield stems from the compound nucleus prior to scission, while only (20 ± 10)% originates from the separated FFs. Hence, this observation corroborates the general findings that the fission process is relatively slow [1], which so far are based mostly on heavy-ion reactions and much lower E^*.

In summary, we have studied the excitation energy dependence of the fission probability in 2.5 GeV proton-induced reactions on Au, Bi, and U. Simulations with the combined intranuclear-cascade–statistical model provide a very satisfying reproduction of the observed evolution of $P_f(E^*)$ with E^*. Prerequisite for this good agreement is that no additional transient delay time is allowed for the fission dynamics at the saddle. Fission thus seems to be decided upon very fast and early in the long deexcitation chain from the highest initial excitations—a conclusion which is, however, at variance with recent conclusions from other provenience [5,6]. The finding of a fast decision to fission is supplemented by the observation that the major part (about 80% at $E^* = 600$–900 MeV) of all alpha particles is evaporated prior to scission or that the entire fission process is, indeed, relatively slow.

The authors thank A. Péghaire from GANIL and L. Pienkowski from Warsaw University for their help during the experiment. The excellent proton beams were provided by the COSY staff and the reliable uranium targets were prepared in the GSI-Darmstadt target laboratory.

*Permanent address: JINR, 141980 Dubna, Russia.
†Electronic address: Jahnke@hmi.de

[1] D. Hilscher and H. Rossner, Ann. Phys. (Paris) **17**, 471 (1992).
[2] P. Fröbrich, Prog. Theor. Phys. Suppl. **154**, 279 (2004).
[3] U. Jahnke *et al.*, Phys. Rev. Lett. **83**, 4959 (1999).
[4] B. Lott *et al.*, Phys. Rev. C **63**, 034616 (2001).
[5] J. Benlliure *et al.*, Nucl. Phys. **A700**, 469 (2002).
[6] B. Jurado *et al.*, Phys. Rev. Lett. **93**, 072501 (2004).
[7] L. Beaulieu *et al.*, Phys. Rev. C **64**, 064604 (2001).
[8] U. Jahnke *et al.*, Nucl. Instrum. Methods Phys. Res., Sect. A **508**, 295 (2003).
[9] C.-M. Herbach *et al.*, Nucl. Instrum. Methods Phys. Res., Sect. A **508**, 315 (2003).
[10] J. Cugnon, Nucl. Phys. **A462**, 751 (1987).
[11] V. E. Viola, K. Kwiatkowski, and M. Walker, Phys. Rev. C **31**, 1550 (1985).
[12] L. N. Andronenko *et al.*, Z. Phys. A **318**, 97 (1984).
[13] L. A. Vaishnene *et al.*, Z. Phys. A **302**, 143 (1981).
[14] A. J. Sierk, Phys. Rev. C **33**, 2039 (1986).
[15] R. J. Charity *et al.*, Nucl. Phys. **A483**, 371 (1988).
[16] K. Siwek-Wilczynska *et al.*, Phys. Rev. C **48**, 228 (1993).